Progress In Electromagnetics Research C, Vol. 108, 103–114, 2021

Reconfigurable Uniform Impedance Active Bandpass Filter Using Coupled Lines for L-Band Satellite Communication

Shikha S. Sharma* and Anjini K. Tiwary

Abstract—This work presents the design and implementation of a four-section reconfigurable uniform impedance resonator (UIR) active filter. UIR active filter consists of $\lambda_g/4$ microstrip line resonators cascaded in series with parallel coupled lines (PCLs). An additional quarter wavelength section is added to the coupled line quarter wave resonator section and gives flexibility in the coupling length. The proposed active filter provides a gain as a means of compensation to loss incurred by passive circuitry. In addition, it gives high selectivity (-70 dB) and wide stopband. The wide stopband is the result of suppression of spurious frequencies which is accomplished by using shunt stub resonators at appropriate locations in the active filter. The bandwidth reconfigurability is achieved by varying the bias currents of the active devices as well as by tuning the varactor diodes. The UIR concept with active matching is implemented on an FR4 substrate ($\varepsilon_r = 4.4$), with passband gain of around 15 dB at 1.3 GHz, and out of band rejection is better than -35 dB at twice the centre frequency of 1.3 GHz.

1. INTRODUCTION

In the midst of the constantly growing demand for reconfigurable bandpass filters, the applications of reconfigurable bandpass microwave active filter having good selectivity are quite popular. The broadband application is renewing the interest in the design of planar broadband filters with low loss, compact size, high suppression of spurious responses, and improved stopband performances. Several papers have been reported with different ways to suppress frequency at second multiple of harmonics [1–4]. The use of half wavelength coupled line open ended resonators [5] coupled to sections of the conventional parallel coupled bandpass filter introduces transmission zero to suppress spurious frequencies. In order to compensate the difference in phase velocities of even and odd modes, a corrugated structure [6] is used in coupled line which facilitates the travelling path for odd mode. Coupled lines with unequal plane apertures also compensate unequal phase velocities [7]. In [8–12], it is shown that an over-coupled resonator and increase in image impedance is responsible for extending phase length of the odd mode to compensate the difference in the phase velocities which further causes suppression of the spurious frequencies.

In this paper, a four-section bandwidth reconfigurable bandpass filter using quarter wave coupled lines cascaded with extra lines at its input and output is designed. The responses at spurious frequencies are suppressed by incorporating two resonating stubs loaded with varactor diodes in the second and third sections of the filter as well as by embedding the amplifiers between the first and second resonators and third and fourth resonators. The loss of the passive mode of the filter is compensated by the gain of the amplifiers of the active filter. The introduced amplifier also brings about active matching or buffering and amplification. This innovative integration of active circuits with a passive parallel coupled line (PCL) filter gives bandwidth reconfigurability, higher selectivity of resonant band, and increases

Received 1 September 2020, Accepted 22 December 2020, Scheduled 6 January 2021
* Corresponding author: Shikha Swaroop Sharma (sharmashikha72@gmail.com).
The authors are with the Department of Electronics and Communication, Birla Institute of Technology, Mesra, Ranchi, Jharkhand 835215, India.

the suppression of spurious modes along with achieving a wide stopband. In addition, the fabricated structure shows the same results as simulated one.

2. DESIGN OF ACTIVE FILTER

A four-section conventional PCL microstrip bandpass filter has been designed initially on an FR4 substrate at 1.3 GHz in microstrip configuration. In the simulation, it is seen that in the inhomogeneous microstrip configuration the phenomenon of second harmonics spurious response takes place which occurs due to the unequal phase velocities of the even and odd modes. In a homogenous transmission line system (stripline), the $\lambda_g/2$ lengths at resonant frequencies of both even and odd modes are equal, therefore creating a zero in the filter response at these harmonic frequencies. However, the inhomogeneous nature of microstrip does not allow the $\lambda_g/2$ lengths of the even and odd modes at resonant frequencies to be equal, consequently leading to a non-zero response at multiple or harmonics of the fundamental frequency considered for the filter design.

Figure 1 shows the design of a modified PCL filter, i.e., Uniform Impedance Resonator Filter by adding $\lambda_g/4$ line lengths at the input and output of the conventional $\lambda_g/4$ PCL resonator line in order to control and increase coupling factor of the resonator. The main aim of this work is to suppress the spurious response to increase the stopband bandwidth and to obtain the gain in the passband along with bandwidth reconfigurability which is, to the best of our knowledge, not reported yet using UIR. This has been achieved by embedding the amplifiers into the four sections configuration of UIR filter and using two varactor loaded shunt stubs in between the sections as shown in Fig. 2. Embedding the amplifiers and loading with varactor loaded shunt stubs are described in Sections 2.1 and 2.2.

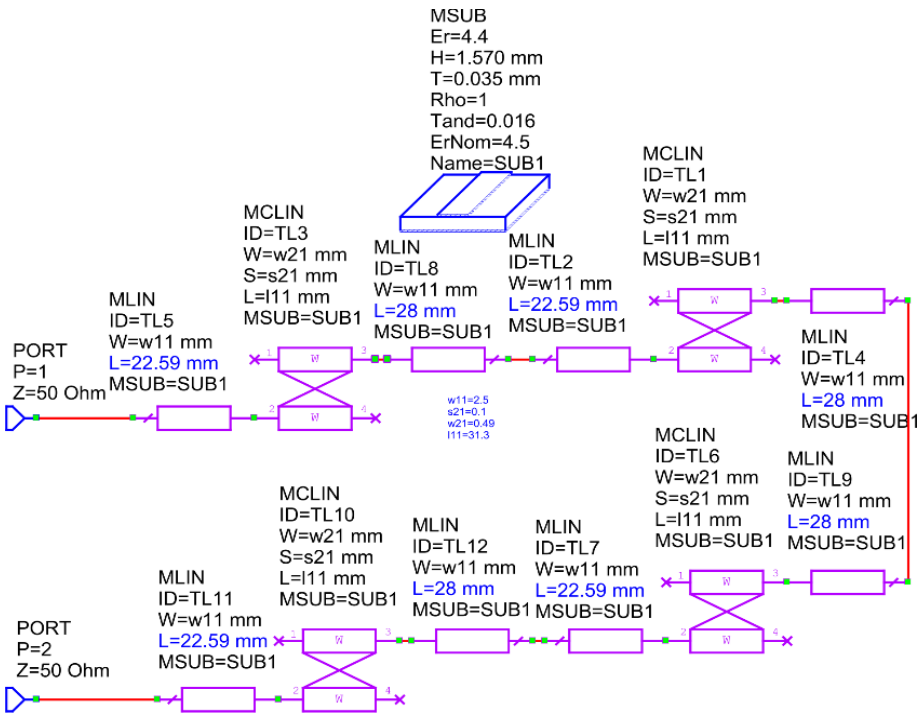

Figure 1. Modified PCL resonator filter.

2.1. Embedding Amplifier

An amplifier using a NEC38018 transistor is designed and embedded between two modified PCL (uniform impedance) resonators. In the overall filter circuit of four modified PCL (uniform impedance) resonators, therefore two amplifiers are embedded in all.

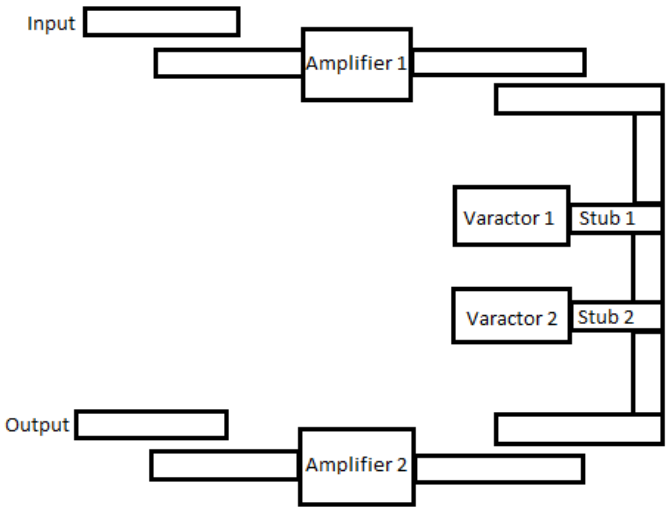

Figure 2. Block diagram of active filter.

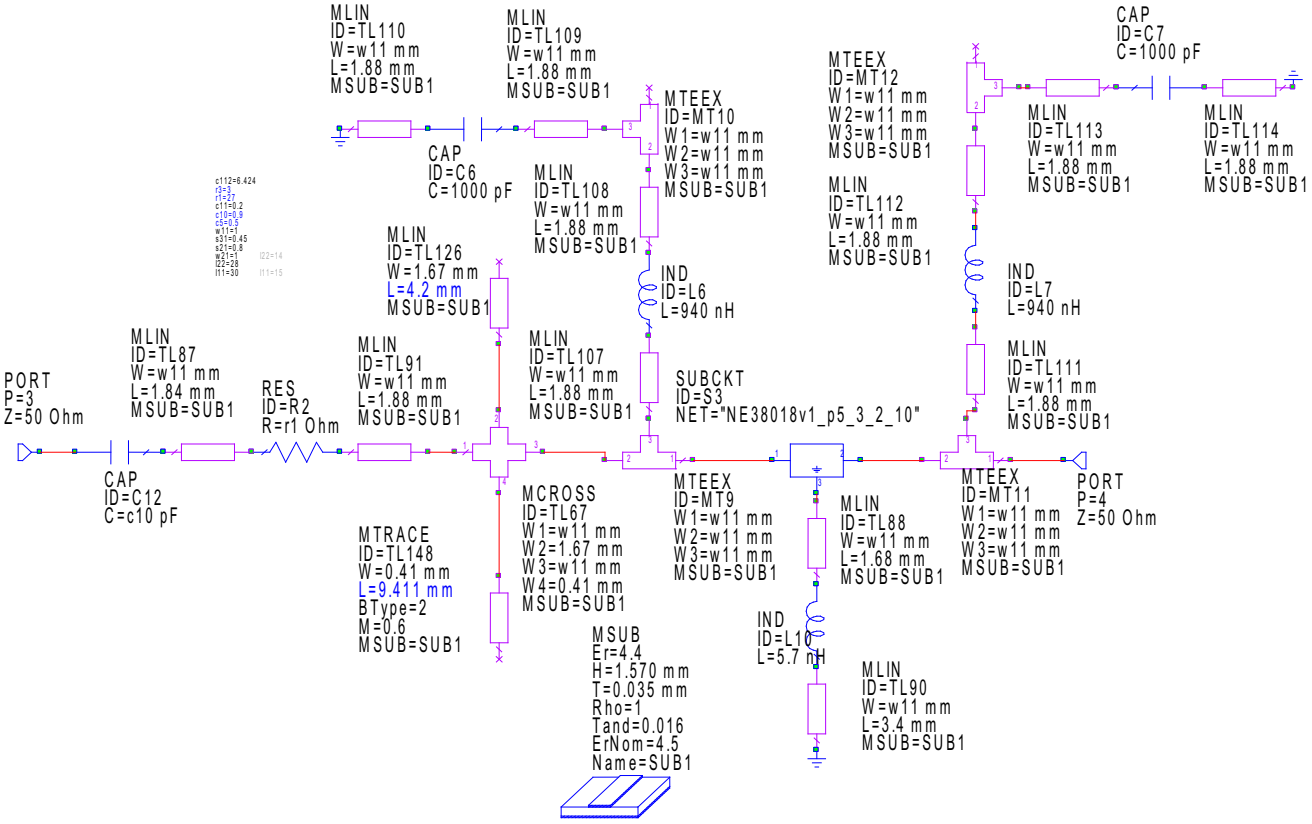

Figure 3. Complete equivalent schematic of the amplifier with biasing and stability circuit.

The amplifier (NEC38018) is biased at $I_d = 10\,\text{mA}$, $V_{ds} = 3\,\text{V}$, and stabilized by using a resistive element in series with gate of the transistor as well as by connecting an inductor or transmission line with the source as a series feedback element. Biasing of the transistor is achieved by using a choke coil ($\sim 940\,\text{nH}$) in shunt with gate and drain. The gate and drain supplies are bypassed by $1\,\mu\text{F}$ capacitors respectively as shown in Fig. 3. The output impedance of the input resonator is almost conjugately

matched with input of the amplifier. Similarly, output impedance of the amplifier can be seen to be matched with the input of the second resonator and likewise for the second amplifier. Without amplifier, occurrence of the spurious frequency response can be observed from 2 to 4 GHz.

2.1.1. Generalized Theory of Modified PCL with Embedded Amplifier

In Fig. 4, which displays the UIRs and embedded amplifiers, the shunt resonance takes place at the output of the amplifier because admittance seen looking into the output of the amplifier could be obtained equal to zero.

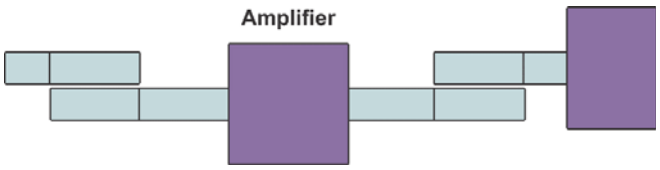

Figure 4. Schematic of the modified PCL.

Using this condition of resonance and conjugate matching at the input and output of the transistor, various design steps of the amplifier design in modified PCL resonator environment are given below.

1. Total $ABCD$ parameters of the designed modified PCL resonator are found.
2. Find the output impedance at centre frequency from $ABCD$ parameters calculated in Eq. (2) (Fig. 5(a)). This output impedance becomes the source impedance (Z_s) to the input matching network of the amplifier.
3. Find the output admittance of the transistor at centre frequency which is capacitive in nature.
4. Tune the output capacitive susceptance with inductive susceptance at $f = 1.3$ GHz (centre frequency) as shown in Fig. 5(c). This forms the output matching network which creates the

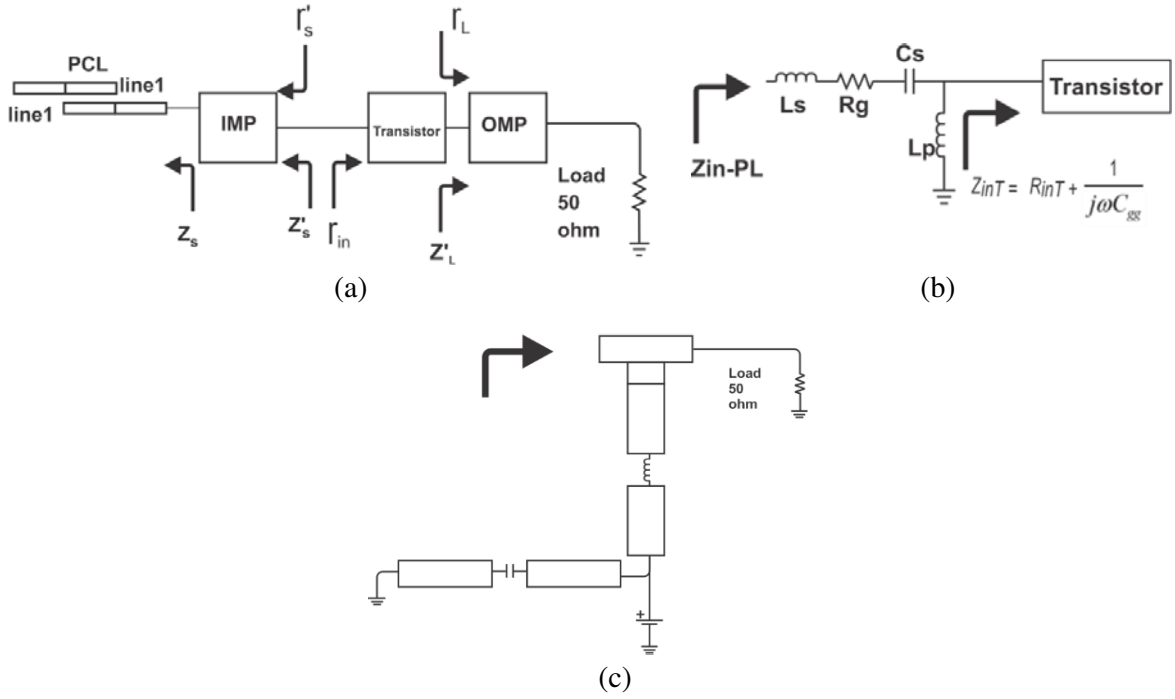

Figure 5. Design schematics of (a) resonators with embedded amplifier, (b) input and (c) output matching networks.

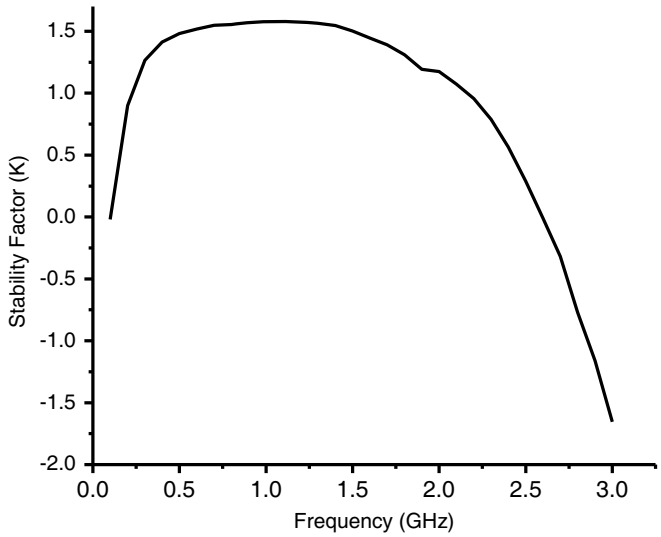

Figure 6. Stability plot of the amplifier.

condition of $\mathrm{Im}[Y_{in}] = 0$ at the output plane of the amplifier.

5. Find Γ_L from the input impedance of output matching network and find Γ_{in} at the input of transistor as shown in Fig. 6(a).
6. As depicted in Fig. 5(a), $\Gamma'_s = \Gamma^*_{in}$ which is a condition for conjugate matching and maximum power transfer at the input of the transistor. $\Gamma's$ is a function of Z_s, series R_g, series capacitor C_s, series inductor L_s and an inductor L_p placed in parallel to the input of the transistor (see Fig. 5(b)). It has one real part, and the other is an imaginary part.

Note that number of components in the input matching network is more than the number of equations for finding their values, and small signal equivalent of input side of the transistor is also considered at low frequency where $(1/j\omega C_{gd})$ can be considered approaching infinity so that input impedance (Z_{inT}) of the transistor is $Z_{inT} = R_{inT} + 1/(j\omega C_{gg})$. Use the $[ABCD]$ parameters of unit PCL (Fig. 1) and the generalized equation of $[ABCD]$ parameters of a transmission line (Eq. (1)).

$$[ABCD]_{\text{line1}} = \begin{bmatrix} \cos\vartheta_1 & jZ_o \sin\vartheta_1 \\ jY_o \sin\vartheta_1 & \cos\vartheta_1 \end{bmatrix} \tag{1}$$

The total $[ABCD]$ parameters of modified PCL is

$$[ABCD]_{\text{Total}} = [ABCD]_{\text{line1}} \cdot [ABCD]_{\text{PCL}} \cdot [ABCD]_{\text{line1}} \tag{2}$$

$$Z_s = \frac{D \cdot 50\,\text{ohm} + B}{C \cdot 50\,\text{ohm} + A} = R_s + jX_s \tag{3}$$

Referring to Fig. 5(a), the terms $\Gamma s'$, Γ_L, Γ_{IN} are

$$\Gamma_{IN} = S_{11} + \frac{S_{12}S_{21}\Gamma_L}{1 - \Gamma_L S_{22}} \quad \Gamma'_S = \frac{Z'_S - Z_o}{Z'_S + Z_o} \quad \Gamma_L = \frac{Z'_L - Z_o}{Z'_L + Z_o} \tag{4}$$

where $Z_s = R_s + jX_s$, $Z'_s = (R_s + R_g) + j(X_s - X_{cs} + \omega L_s)||j\omega L_p$, $X_{cs} = 1/j\omega C_s$.

From Fig. 5(b), it can be found

$$Z_{in-L_P} = \frac{R_g + (\omega L_{p1})^2}{R_p} + j\frac{(\omega\,(L_{p1} + L_s) - 1)}{\omega C_s} \tag{5}$$

where,

$$L_{p1} = \mathrm{Im}[(j\omega L_P) \parallel (R_{inT} + (1/j\omega C_{gg}))], \quad R_p = \frac{1}{R_{inT}(\omega C_{gg})^2} \tag{6}$$

L_{p1} is the inductance seen by C_s when looking towards the transistor. Therefore, when the input of transistor is matched one obtains,

$$\frac{R_g + (\omega L_{p1})^2}{R_p} = R_s \text{ and } \omega (L_{p1} + L_s) = \frac{1}{\omega C_s} \tag{7}$$

$$\Gamma_s' = \Gamma_{in}^* \tag{8}$$

The equations from Eqs. (4) to (8) are solved to find R_g, L_s, C_s and L_p. R_g are used for incorporating stability (Fig. 6) into the amplifier, and L_s is used in the form of inductive interconnects between R_g and C_s as well as between C_s and L_p.

All these equations can be solved using AWR MWO, and the resonance occurring at the output of the amplifier is given in Results and Discussion section (Fig. 9).

The amplifier not only amplifies the signal, converts the loss of the filter into gain, but also contributes towards the reconfigurability of active filter's bandwidth due to the capacitive loading of the modified PCL resonators by the amplifiers.

The pass and stop bands of the filter are further improved when amplifier is embedded between two modified PCL resonators. It is mostly due to the same amplifier matching frequency and modified PCL resonant frequency. Note that the strong magnetic coupling between coupled lines can be invoked at the resonant frequency which results into a high Q resonance and a large current flow into the amplifier through maximum power transfer at resonance due to conjugate matching to the transistor at its input and output at the resonant frequency. This inhibits signal propagation in the vicinity of that frequency allowing the rejection of undesired passbands. This requires proper tuning of the modified PCLs. There is added rejection of the signals at the undesired frequencies due to mismatch caused between the input/output matching network of the amplifier and the modified PCLs causing further suppression of the spurious responses. The amplifier would bring spurious suppression from -5 dB to -25 dB. Note that reducing gain helps in increasing out of band attenuation thus suppressing spurious responses in stopband.

2.2. Shunt Stubs Loaded with Varactor Diodes

Further improvement in suppression of spurious response has been achieved by employing two stubs loaded with varactor diodes placed in shunt between stages 2 and 3. The spurious suppression from -20 dB to -40 dB has been achieved by such an arrangement, but a noticeable loss of ~ 2.5 dB happens in the passband. The varactors diodes can be tuned for bringing about bandwidth reconfigurability by varying the capacitive loading of the modified PCL resonators apart from the enhancement of out of band rejection.

3. RESULTS AND DISCUSSIONS

The modified PCL resonators with four sections have been designed having the amplifier circuits integrated into them and varactor loaded stubs placed between Sections 2 and 3 as shown in Fig. 7(a). Figs. 7(b)–(c) show the measured results. Results show that center frequency of the active filter is around 1.3 GHz with the passband gain around 15 dB. The amplifiers convert the loss in the passband of passive mode of the bandpass filter (~ -2 dB) into the gain of the active filter (~ 15 dB). The amplifiers are innovatively integrated between the two modified PCL resonators. The amplifiers are conjugately matched to these modified PCL resonators at frequency of resonance, so that at this central frequency not only the filter resonates to have maximum gain in the passband but, at the same time, the amplifiers also mismatch at out of the passband frequencies to suppress the spurious response by increasing attenuation in the stopbands (see Figs. 7(b)–(c)). As already discussed, approximate conjugate matching is achieved at the input and output of each amplifier with respect to resonator's output and input impedances, respectively. Thereby, each amplifier also acts as a buffer between two resonators. The suppression of the spurious frequency (harmonics) response between 2 and 3 GHz is because of the high selectivity and reverse isolation of the amplifier. Secondly, the amplifiers also play an important role in reconfigurability of the bandwidth. The amplifiers are made stable throughout the frequency band from DC to transition frequency of the transistor (f_t) by making stability factor

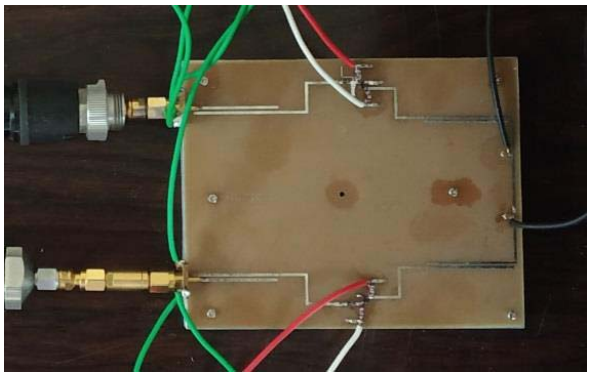

(a)

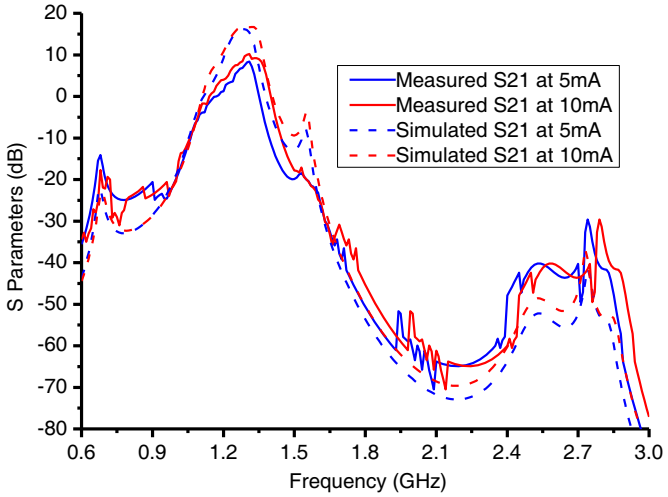

(b)

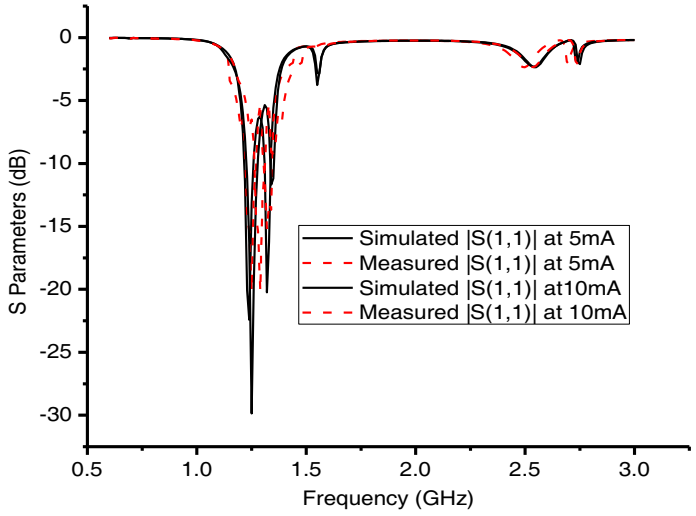

(c)

Figure 7. (a) Fabricated active filter, simulated and measured results of (b) $|S(2,1)|_{\mathrm{dB}}$ and (c) $|S(1,1)|_{\mathrm{dB}}$.

$K > 1$ and by making $B1$ (auxiliary stability factor) a positive quantity. After biasing the amplifiers for suitable gate and drain voltages, the bandwidth reconfigurability about more than 200 MHz could be achieved at the 3 dB bandwidth which expands from 0.23 GHz to 0.287 GHz. As already mentioned, the UIRs improve the return loss and control coupling. The return loss of the active filter is found to be better than 20 dB from simulations which are further verified using measurements. Properties of the designed amplifier, its case study, and bandwidth reconfigurability of the active filter are stated in the subsequent sections.

3.1. Properties of Amplifier in Active Filter

The following is the properties of the embedded amplifiers —

1. It approximately conjugately matches, at its input, with the output of the first resonator as shown in Fig. 8.

2. Output planes of the amplifiers while looking into the output of the amplifiers give $Y_{in} = 0$, i.e., the planes display shunt resonances as shown in Fig. 9. The plane between two varactor loaded stubs

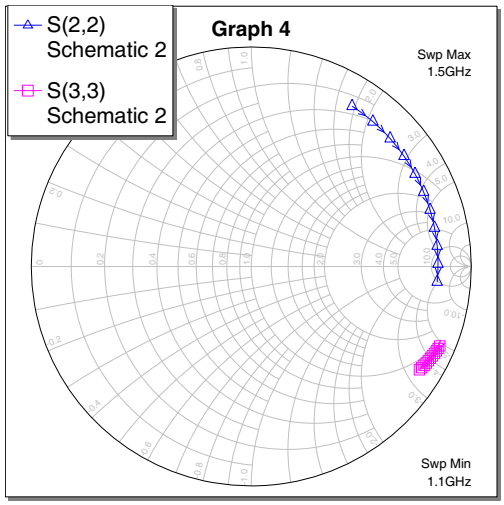

Figure 8. Conjugate matching of amplifier with resonator.

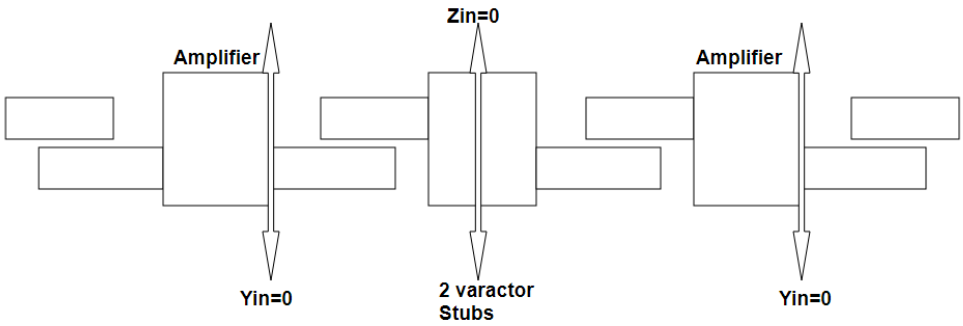

Figure 9. Planes for shunt and series resonances.

between Sections 2 and 3 is a plane of zero impedance, i.e., $Z_{in} = 0$. So alternative planes of $Y_{in} = 0$ and $Z_{in} = 0$ constitute a bandpass filter response as shown in Fig. 10.

3. While comparing $[S_{21}]_{\text{dB}}$ of passive filter and $[S_{21}]_{\text{dB}}$ of the active filter with varactor loaded stubs (Fig. 11), it can be seen that the active filter with varactor loaded stubs is without any spurious response and with better in band selectivity. This happens along with better out of band rejection than that of the passive filter which is without any varactor loaded stub. Note that Fig. 11 closely follows Fig. 10 for input admittance and input impedance plots.

4. Initial simulation is carried out using small signal S-parameters at bias $V_{gs} = -0.58\,\text{V}$ and $V_{ds} = 2.16\,\text{V}$ which has also been verified using measurements. However, to study the compression of the output signal in the device and the input power handling capability of the active filter along with its effects on the circuit performances, the nonlinear model of the device has been, used and the observations are tabulated in Table 1. When the resistance (R_g) in series of the gate in the amplifier is $36\,\Omega$, input power could be increased from $-5\,\text{dBm}$ to $2.75\,\text{dBm}$ without any oscillation problem in the amplifiers. With the increase of input power, the output power gain gets continuously compressed from $17.33\,\text{dB}$ to $14.59\,\text{dB}$ as shown in Table 1 while small signal gain remains more or less constant at $\sim 17.03\,\text{dB}$ after slightly degrading from $20.36\,\text{dB}$ to $17.33\,\text{dB}$. Similarly, input reflection coefficient, i.e., $[S_{11}]_{\text{dB}}$, is also constant at $\sim 16.87\,\text{dB}$. The oscillation starts taking place at $\sim 0.9\,\text{GHz}$ beyond $2.75\,\text{dBm}$ of input power.

To increase the power up to $5\,\text{dBm}$, R_g is increased to $100\,\Omega$ at the cost of a small signal gain and power gain. The small signal gain at $Pin = 5\,\text{dBm}$ is decreased to $14.18\,\text{dB}$, and the power gain falls to $12.17\,\text{dB}$. Again, beyond $5\,\text{dBm}$ of input power oscillation starts at the same frequency of $0.9\,\text{GHz}$.

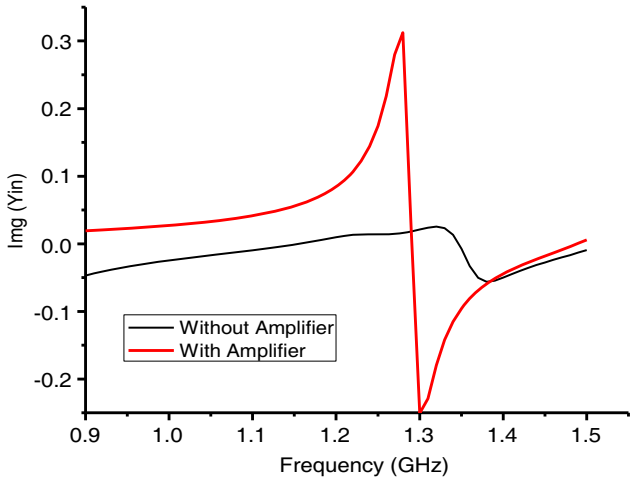

Figure 10. Simulated input impedance and admittance plots.

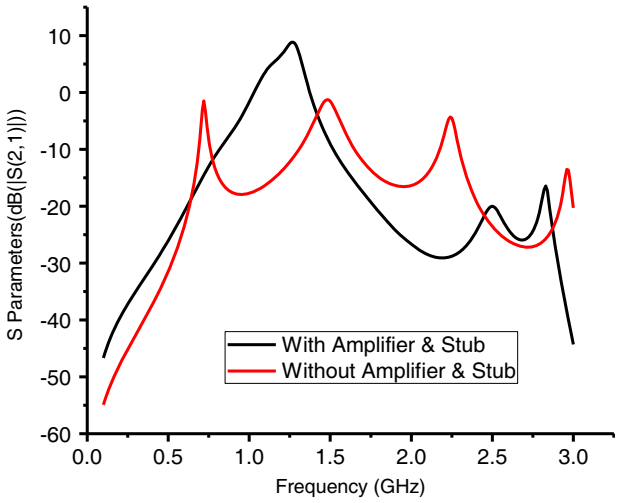

Figure 11. Comparative $|S_{21}|_{\mathrm{dB}}$ response of the filter with and without the amplifier and varactor loaded stubs.

Table 1. Circuits performance with the increase of input power using nonlinear model at frequency (1.3 GHz).

$\boldsymbol{R_g = 36\,\Omega}$				
Input Power (dBm)	dB $\lvert S(1,1)\rvert$	dB $\lvert S(2,1)\rvert$	Power Gain (dB)	Total output Power (dB)
−5	−16.87	20.26	17.33	15.32
−10	−16.87	17.33	19.16	9.456
2	−17.02	17.03	15.26	17.44
2.5	−16.87	17.03	14.76	17.03
2.75	−16.87	17.51	14.59	17.51
$\boldsymbol{R_g = 100\,\Omega}$				
5	14.36	14.18	12.17	17.29
$\boldsymbol{R_g = 600\,\Omega}$				
10	−19.43	8.9	2.332	12.76

To bring about the input power capability of 10 dBm, R_g is increased to 600 Ω for which dB $[S_{21}]$ drops to 8.9 dB, and power gain drops drastically to 2.332 dB. So, as input power increases, output power decreases continuously as the output load for transistors' power matching changes continuously. Also, the amplifiers are not matched for optimum power at the output. Therefore, linearity of the amplifier is not seen when increase in the input power takes place. To avoid oscillations and to increase input power handling, R_g is increased which is also at the cost of output power and power gain. Though output power is still around $\sim$ 12 dBm, power gain suffers severely. So, device acts nonlinearly even at the beginning of the input power increase.

3.2. Reconfigurability

The fabricated structure is shown in Fig. 7(a). The reconfigurability as shown in Figs. 7(b)–(c) is achieved by changing the bias voltages of transistor and varactor diodes' capacitances. The amplifiers capacitively load the modified PCL resonators causing the bandwidth shrinkage. Therefore, as bias voltages change, the capacitive load also changes which brings about the change in bandwidth, and thus the bandwidth reconfigurability takes place. The varactor (capacitive) loading of stubs also produces

Table 2. Bandwidth reconfigurability at different bias and varactor capacitances.

V_{gs} (V)	V_{ds} (V)	Varactor2 (pF)	Varactor3 (pF)	Bandwidth (GHz)
−0.58	3.079	5.58	2.46	0.271
−0.58	3.079	3	5.4	0.304
−0.417	1.172	3	5.4	0.44
−0.417	1.172	4.34	2.78	0.524

the same result and increases the bandwidth reconfigurability as shown in Table 2 for completeness. The varactor loading also helps in suppression of spurious responses by enhancing the odd mode phase length which reduces the difference between even and odd mode phase velocities. This helps in providing wide stopband performance.

3.3. Case Study of Series RC Dependence of Reconfigurability

The effect of series combination of RC used in designing the amplifier is dully studied by virtue of its position and value of series capacitance on the phenomenon of bandwidth reconfigurability. The three positions of RC taken in the amplifier circuit are:

Table 3. Effect of series capacitance values of the RC combination on reconfigurability.

V_{gs} (V)	V_{ds} (V)	Var2 (pF)	Var3 (pF)	Transistor 1 Cap. (pF)	Transistor 2 Cap. (pF)	Bandwidth (GHz)
−0.58	3.079	5.58	2.46	0.8	0.84	0.271
−0.41	1.172	4.34	2.78	0.549	8.41	0.570

Table 4. State-of-the-art performance comparisons.

Ref. No	Reconfigurable Parameters	S_{11} (dB)	S_{21} (dB)	Device
[13]	Bandwidth	−15	−1.1	PIN diode
[14]	Bandwidth	−10	−1.9	Varactor and PIN diode
[15]	Bandwidth and Frequency	−15 to −18	−2 to −5	Varactor and PIN diode
[16]	Bandwidth and Frequency	−10	−3	PIN diode
[17]	Bandwidth	−15	−0.42	Varactor diode
[18]	Frequency	−20	−0.6	Varactor diode
[19]	Bandwidth and Frequency	−14 to −10	−2.41	inter-resonator coupling structures
[20]	Bandwidth	−15	−2	PIN diode
[21]	Bandwidth and Frequency	−22	−1.5	Varactor diode
[22]	Bandwidth	−30	−1.5	PIN diode
This work	**Bandwidth**	**−17**	**10**	**Transistor and Varactor**

1. At the input of the gate in both the amplifiers.
2. At the output of the drain in both the amplifiers.
3. At the input of the gate in the first amplifier and at the output of the drain of the second amplifier.

For case-1 and case-3, amplifiers are stable with respect to bias voltages for given values of series resistances. However, case-2 is very sensitive with respect to the bias voltages as the amplifier becomes unstable. Case-1 gives the maximum reconfigurability with respect of change in bias voltages in both the amplifiers. Case-3 has been taken for a trade-off between S_{11} and less reconfigurability. Here, we follow this trade-off for fabricating our circuit on an FR4 substrate. If our prime requirement is reconfigurability, then our studies show that case-1 is more suited to get high reconfigurability. Table 3 gives the view of the effect of series capacitance values of the RC combination on reconfigurability. Finally, performances of the proposed device are compared with other state-of-the-art devices and tabulated in Table 4 for completeness.

4. CONCLUSION

An electronically tunable coupled line bandpass filter integrated with varactor diodes' loaded stubs and the amplifiers is proposed and demonstrated. By changing the bias of amplifier reconfigurability of more than ~ 200 MHz has been obtained. In addition, the spurious frequencies have been suppressed by employing varactor loaded stubs and the amplifiers themselves. This new concept will help in obtaining bandwidth reconfigurability in tightly coupled microstrip lines. The primary objective of this work is to obtain a spurious free bandpass filter with bandwidth reconfigurability. For resonator being PCL, spurious frequencies are generated at integer multiples of fundamental central frequency which is 1.3 GHz. $\lambda_g/4$ resonators are cascaded with PCL resonator to vary coupling length. While accomplishing this, wider bandwidth is achieved at the cost of insertion loss. The loss of the passive mode of the filter, i.e., the filter without the amplifier, is compensated by using the amplifier (NEC38018) connected between the various resonators of the filter circuit.

REFERENCES

1. Matthaei, G. L., L. Young, and E. M. T. Jones, *Microwave Filters, Impedance-matching Network and Coupling Structures*, McGraw-Hill, 1964.
2. Phromloungsri, R., S. Patisang, K. Srisathit, and M. Chongcheawchamnan, "A harmonic-suppression microwave bandpass filter based on an inductively compensated microstrip coupler," *Asia-Pacific Microw. Conf. Proceedings*, Vol. 5, No. 1, 0–3, 2005.
3. Makimoto, M. and S. Yamashita, *Microwave Resonators and Filters for Wireless Communication — Theory and Design*, Springer, 2001.
4. Chang, C. Y. and T. Itoh, "A modified parallel-coupled filter structure that improves the upper stopband rejection and response symmetry," *IEEE Trans. Microw. Theory Tech.*, Vol. 39, No. 2, 310–314, 1991.
5. Hong, S. and K. Chang, "A parallel-coupled microstrip bandpass filter with suppression of both the 2nd and the 3rd harmonic responses," *IEEE MTT-S Int. Microw. Symp. Dig.*, 365–368, 2006.
6. Kuo, J. T., W. H. Hsu, and W. T. Huang, "Parallel coupled microstrip filters with suppression of harmonic response," *IEEE Microw. Wirel. Components Lett.*, Vol. 12, No. 10, 383–385, 2002.
7. Sun, S. and L. Zhu, "Coupling dispersion of parallel-coupled microstrip lines for dual-band filters with controllable fractional pass bandwidths," *IEEE MTT-S Int. Microw. Symp. Dig.*, 2195–2198, 2006.
8. Jiang, M., M. H. Wu, and J. T. Kuo, "Parallel-coupled microstrip filters with over-coupled stages for multispurious suppression," *IEEE MTT-S Int. Microw. Symp. Dig.*, 687–690, 2005.
9. Pozar, D. M., *Microwave Engineering*, 2nd Edition, Wiley, 1998.
10. Ye, C.-S., Y.-K. Su, M.-H. Weng, C.-Y. Hung, and R.-Y. Yang, "Design of the compact parallel-coupled lines wideband bandpass filters using image parameter method," *Progress In Electromagnetics Research*, Vol. 100, 153–173, 2010.

11. Perhirin, S. and Y. Auffret, "A low consumption electronic system developed for a 10 km long all-optical extension dedicated to sea floor observatories using power-over-fiber technology and SPI protocol," *Microw. Opt. Technol. Lett.*, Vol. 55, No. 11, 2562–2568, 2013.
12. Chang, Y. C., C. H. Kao, M. H. Weng, and R. Y. Yang, "Design of the compact wideband bandpass filter with low loss, high selectivity and wide stopband," *IEEE Microw. Wirel. Components Lett.*, Vol. 18, No. 12, 770–772, 2008.
13. Arain, S., P. Vryonides, M. A. B. Abbasi, A. Quddious, M. A. Antoniades, and S. Nikolaou, "Reconfigurable bandwidth bandpass filter with enhanced out-of-band rejection using π-section-loaded ring resonator," *IEEE Microw. Wirel. Components Lett.*, Vol. 28, No. 1, 28–30, 2018, doi: 10.1109/LMWC.2017.2776212.
14. Bi, X. K., X. Zhang, S. W. Wong, S. H. Guo, and T. Yuan, "Design of notched-wideband bandpass filters with reconfigurable bandwidth based on terminated cross-shaped resonators," *IEEE Access*, Vol. 8, 37416–37427, 2020, doi: 10.1109/ACCESS.2020.2975379.
15. Kheir, M., T. Kröger, and M. Höft, "A new class of highly-miniaturized reconfigurable UWB filters for multi-band multi-standard transceiver architectures," *IEEE Access*, Vol. 5, 1714–1723, 2017, doi: 10.1109/ACCESS.2017.2670526.
16. Kingsly, S., et al., "Compact frequency and bandwidth reconfigurable microwave filter," *Wirel. Pers. Commun.*, Vol. 115, 1755–1768, 2020, doi: 10.1007/s11277-020-07652-0.
17. Kingsly, S., et al., "Bandwidth reconfigurable microwave filter using stepped impedance c-shaped resonator," *Microw. Opt. Technol. Lett.*, 1–5, February 2020, doi: 10.1002/mop.32616.
18. Kumar, L. and M. S. Parihar, "A compact reconfigurable low-pass filter with wide-stopband rejection bandwidth," *IEEE Microw. Wirel. Components Lett.*, Vol. 28, No. 5, 401–403, 2018, doi: 10.1109/LMWC.2018.2823001.
19. Lee, T. C., W. Yang, and D. Peroulis, "Reconfigurable filter design using resonators as coupling structures," *2015 IEEE MTT-S Int. Microw. Symp., IMS 2015*, Vol. 2, 2–5, 2015, doi: 10.1109/MWSYM.2015.7166884.
20. Masood, M. H. and S. B. Suseela, "Compact band-pass filter with reconfigurable X-band using stepped impedance resonator and folded structure," *J. Eng.*, Vol. 2018, No. 3, 162–165, 2018, doi: 10.1049/joe.2017.0796.
21. Schuster, C., et al., "Performance analysis of reconfigurable band-pass filters with continuously tunable center frequency and bandwidth," *IEEE Trans. Microw. Theory Tech.*, Vol. 65, No. 11, 4572–4583, 2017, doi: 10.1109/TMTT.2017.2742479.
22. Vryonides, P., S. Nikolaou, S. Kim, and M. M. Tentzeris, "Reconfigurable dual-modeband-pass filter with switchable bandwidth using PIN diodes," *Int. J. Microw. Wirel. Technol.*, Vol. 7, No. 6, 655–660, 2015, doi: 10.1017/S1759078714000932.